AO Observations of Three Powerful Radio Galaxies

W. De Vries, W. van Breugel, A. Quirrenbach

August 1, 2002

U.S. Department of Energy
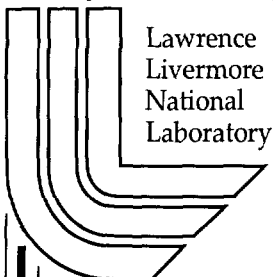
Lawrence
Livermore
National
Laboratory

AO Observations of Three Powerful Radio Galaxies

Wim de Vries[a], Wil van Breugel[a], and Andreas Quirrenbach[b]

[a]IGPP-LLNL, 7000 East Ave, Livermore, CA 94550, USA
[b]Univ. of California at San Diego, San Diego, USA

ABSTRACT

The host galaxies of powerful radio sources are ideal laboratories to study active galactic nuclei (AGN). The galaxies themselves are among the most massive systems in the universe, and are believed to harbor supermassive black holes (SMBH). If large galaxies are formed in a hierarchical way by multiple merger events, radio galaxies at low redshift represent the end-products of this process. However, it is not clear why some of these massive ellipticals have associated radio emission, while others do not. Both are thought to contain SMBHs, with masses proportional to the total luminous mass in the bulge. It either implies every SMBH has recurrent radio-loud phases, and the radio-quiet galaxies happen to be in the "low" state, or that the radio galaxy nuclei are physically different from radio-quiet ones, i.e. by having a more massive SMBH for a given bulge mass.

Here we present the first results from our adaptive optics imaging and spectroscopy pilot program on three nearby powerful radio galaxies. Initiating a larger, more systematic AO survey of radio galaxies (preferentially with Laser Guide Star equipped AO systems) has the potential of furthering our understanding of the physical properties of radio sources, their triggering, and their subsequent evolution.

Keywords: Adaptive Optics, Radio Galaxies, AGN

1. INTRODUCTION

Powerful radio galaxies provide a convenient way to investigate the evolution of very massive galaxies over a large range in redshift. Color properties of their host galaxies have been found to be remarkably well represented by passively evolving stellar systems, with typical masses of $5 - 10$ L_*.[1,2] Comparison with high redshift field galaxies[3] confirms that radio galaxies form indeed the high-luminosity envelope. Inferred formation redshifts for these systems have been as high[4] as $z_f > 10$, implying that by a redshift of 1 to 2, emission from these galaxies is dominated by an old (> 5 Gyr) stellar population. It is this homogeneity in population (and emission) properties that makes the near-IR Hubble K-z relation so tight.

Radio galaxy morphologies, when imaged at rest-frame optical wavelengths, often show spectacular, clumpy structures aligned with the radio source axes. This "alignment effect" appeared at odds with the passive evolution inferred from the near-IR K-z diagram. Its exact nature has remained unclear and evidence has been found for scattered light from hidden quasar-like AGN, nebular re-combination continuum and even jet-induced star formation.[5]

To investigate the morphological evolution of the stellar populations of radio galaxies with redshift, it is therefore of interest to obtain high spatial resolution at *infrared* wavelengths, where AGN-related emission is fainter and the old stellar population brighter. This effective isolation of just the stellar emission component also provides a useful baseline against which we can interpret the optical HST data. Again, given the rather uniform stellar population, any color-deviations will stand out in a color plot based on combining HST optical and Keck AO near-IR data (cf. Fig. 1). Features, such as dust-lanes, or compact regions of enhanced starformation can be clearly detected against the uniform backdrop of the underlying galaxy. Furthermore, the high resolution near-IR images allows us to extract physically meaningful luminosity profiles, which are much less affected by obscuring dust or AGN related non-stellar emission. Using HST on a large sample of (radio quiet) galaxies, Faber et al.[6] found the shape of the inner galaxy profile to correlate with various physical quantities such as absolute luminosity and central velocity dispersion; provided the profile can be fitted with a "Nuker" profile.[7,8]

Email: devries1@llnl.gov, vanbreugel1@llnl.gov, qui@cassir.ucsd.edu

Up till now, only with HST was the necessary spatial resolution attainable. With the Keck-AO system, this can be improved upon by at least a factor of 4 (cf. Fig. 3). This allows us to intercompare more distant radio galaxy hosts to "normal" ellipticals, which could provide additional clues about why some galaxies are radio emitters and others are not.

In principle high resolution spectroscopy can not only provide us with diagnostic line ratios which constrain ionization mechanisms (i.e., starbursts vs. AGN[9–11]), and absorption properties of circumnuclear features,[12–14] but it can also provide us with accurate measurements of nuclear stellar velocity dispersions using the ^{12}CO near-IR bandhead at 2.29μm restframe.[15, 16] Given the very high spatial (and spectroscopic) resolution of the observations, these will provide nuclear black-hole (BH) mass estimates (analogous to Böker[16] et al.). Values derived this way for our sample can then be compared directly to recent results on the velocity—BH-mass correlation for lower redshift galaxies.[17, 18] However, a combination of instrumental throughput issues beyond $\sim$ 2.4 μm, the anisoplanatism inherent to off-axis correction, and just plain bad weather prevented us from achieving our planned spectroscopic goals.

Either way, both the imaging and spectroscopy parts of the program have yielded insights into the makeup of the stellar systems of the 3 powerful radio galaxies and their place in the elliptical galaxy taxonomy. This illustrates the potential AO can offer us in understanding the onset and subsequent evolution of powerful nuclear radio sources, provided this pilot project is carried out on a much larger sample and in a more complete fashion, ideally with a LGS equipped AO system.

2. OBSERVATIONS

Our target galaxies have been selected from cross-correlations between the NVSS radio catalog, the HST guide star catalog, and the HST archive catalog. Positive hits have been checked against the USNO-A2.0 star catalog, as a fair fraction of the HST guide star catalog consists of non-stellar objects (e.g., galactic nuclei), and we want to make sure there is an AO star present. Furthermore, we have limited the redshift range to $0.015 < z < 0.10$ in order for the ^{12}CO spectroscopic band-head at 2.293 μm not to be redshifted beyond 2.5 μm. The decreasing instrumental response and increase in the thermal background (part of which is instrumental, too) are not well suited for observing beyond this wavelength with the KECK NIRSPEC instrument. The sample and observations are listed in Table 1.

As for the imaging part of the program, the high resolution H and K-band AO images surpass the complementary R-band HST images in resolution. In addition, the combination of the optical and near-IR images (both with < 0.1 arcsecond resolution) provides a powerful tool for investigating the nuclear morphologies of these radio galaxies in unprecedented detail (cf. Fig. 1). The much higher near-IR resolution of the Keck AO system compared to the HST NICMOS cameras makes this possible for the first time.

Of the three radio sources (3C 403, 3C 405, and 3C 452), only 3C 452 was specifically imaged with NIRSPEC's slitviewing camera (SCAM). For this purpose the smallest of the slits (1.3×0.013″) was inserted to minimize the light lost into this slit (and to SCAM), plus the object was dithered across the field of view to further reduce the impact of the slit. The other two sources were mainly spectroscopic targets, and as such the SCAM images suffer from the presence of the "large" 3.96×0.072″ slit which consistently covered the nucleus (since we were interested in the nuclear *spectrum*).

The SCAM camera, a 256^2 HgCdTe NICMOS array, has both a low readout-noise and a high-throughput, and provides with its 0.0172″ pixel scale a 4.4 square arcseconds field of view (cf. NIRSPEC/AO manual). The NIRSPEC spectrograph was operated in low- resolution mode, and resulted in a $\sim$ 12.7Å instrumental resolution at 2.4 μm ($R \approx 1900$), equivalent to a $\sim$ 160 km/s velocity resolution. This matches best the expected velocity dispersion of $\sim$ 500km/s (FWHM) of our objects, while still retaining adequate S/N per resolution element. The high resolution mode of the spectrograph ($R \approx 20000$) would not.

The superb spatial resolution of the AO-NIRSPEC spectrograph allows for an effective isolation of the spectral features related to the AGN from the underlying galaxy. This, in principle, allows for accurate BH-mass assessments (cf. Sect 4).

3. IMAGING OF 3C 452 - A CASE STUDY

The performance of the AO-system declines with distance from the optical axis, but does so rather gracefully. The separation between 3C 452 and the guide star is $\sim 11''$ which is well inside the isoplanatic angle of (up to) $45''$ radius for the Keck system. Based on our observations on 3C 294 earlier in the night,[19] and experiences by other observers,[20] we estimate that the Strehl-ratio for our images declines from the ~ 0.2 for the on-axis case of the guide star, to ~ 0.1 for the radio galaxy itself. Given the rather small point-source component in the galaxy (cf. Sect. 3.3) a direct assessment of the Strehl-ratio is not possible. The FWHM of the core in the K$'$-band image is 55 milliarcseconds however, close to the theoretical resolution limit of a 10m telescope (45 mas at K$'$).

Since our source is well resolved and effectively without an unresolved component, the image resolution is for all practical purposes comparable to the diffraction limit. In other words, even though the Strehl-ratios are only about of 10% of the values of a perfect telescope, the resulting PSF is peaked enough compared to the galaxy profile that its convolution does not significantly degrades the input image. Inversely, since the convolved image is the one we actually obtain, a deconvolution with either a model of actual PSF does not significantly change the image properties. Image profile parameters (cf. Sect. 3.2) between the unconvolved and Richardson-Lucy deconvolved images were identical within their errorbars.

3.1. Morphological Parameters

The H and K$'$-band AO images have a resolution comparable to HST WFPC2 optical images, making it for the first time possible to construct color images which are not affected by resolution effects (like WFPC2 - NICMOS color maps).

Fluxes in each of the images are converted into Watts (νF_ν) before dividing both images. This way the ratio represents a real fractional energy excess. The color maps are plots of the following function:

$$\text{ColorMap} = \frac{1 + f \times \text{CR}_{F702W}[\text{DN/s}]}{1 + \text{CR}_H[\text{DN/s}]} - 1 \tag{1}$$

Table 1. Radio Source Sample + Observational Results

Source Name	Coordinates (J2000)	Redshift	GS Mag.	Separation
3C 403	19 52 15.39 +02 30 28.2	0.0590	10.7	$8''$
3C 405	19 59 25.86 +40 43 50.9	0.05608	12.4	$31''$
3C 452	22 45 48.85 +39 41 15.2	0.0811	10.8	$13''$

Imaging Observations	Filter	
3C 452	H-band	5×300s exposure, 24 Jun 2000 H = 13.5±0.2
3C 452	K$'$-band	5×300s exposure, 24 Jun 2000 K$'$ = 13.4±0.2

Spectroscopic Observations	Filter	
3C 403	NIRSPEC7	4×900s exposure, 09 May 2001 3.96×0.072$''$slit
3C 405	NIRSPEC7	8×900s exposure, 26 Aug 2001 3.96×0.072$''$slit
3C 452	NIRSPEC7	3×1400s exposure, 31 Aug 2001 3.96×0.072$''$slit
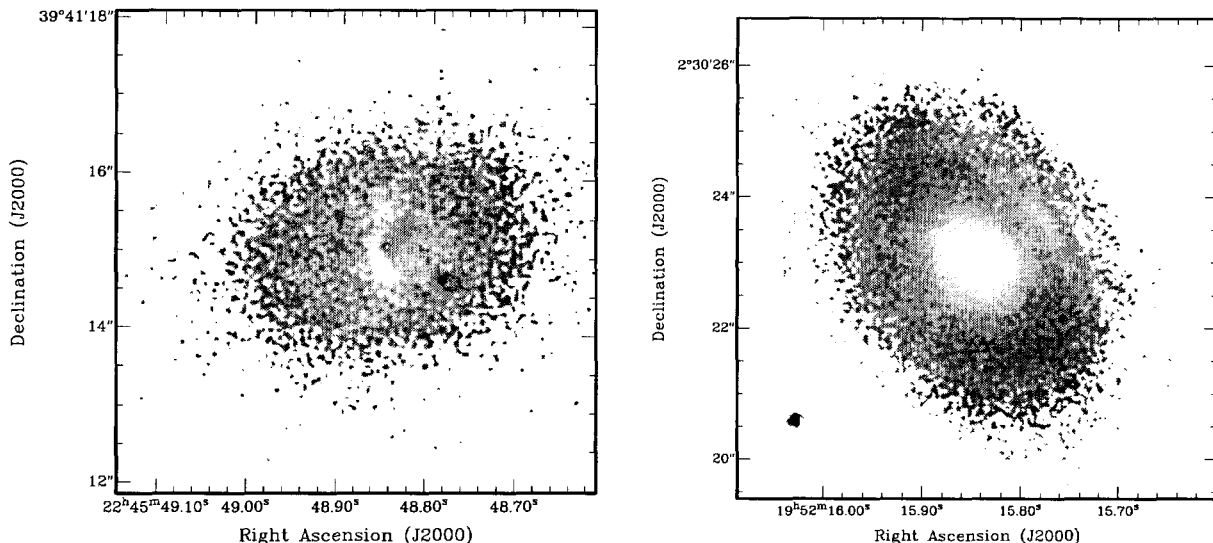
Figure 1. [Left Panel] Color Map of 3C 452. Both the HST WFPC2 image and the KECK-AO H-band image have been renormalized to the same energy flux levels (in units of ergs/s/cm^2/count/pixel). The color coding is as follows: Grey = neutral, White = more energy in H-band, Black = more energy in R-band. Note the prominent dust lane, and the "blue" companion. [Right Panel] Same for 3C 403, with the key distinction that the near-IR data has been modeled, based on actual data. The color of the companion in the lower left corner is undefined: it was not covered by this model.

where the factor f is calculated by normalizing F702W and H-band fluxes to the same energy level, after resampling the F702W pixels onto the smaller H-band pixels (7 H-band pixels per WFPC2 pixel, area-wise). The factor works out to be: $f \approx 50$. The constant 1 has been chosen in such a way as to yield approximately the same standard deviation in the sky as in the original images. This also suppresses large color variations in the noise dominated areas of the map. The colormaps are presented in Fig. 1. For comparison we included a modified color-map for the source 3C 403. Since the slit was so much more prominent in this source, we actually used a model of the near-IR luminosity distribution instead of the actual image to construct the color-map.

The smooth near-IR background luminosity distribution of 3C 452 provides a very good background to offset the optical HST data against. This is quite dramatically demonstrated by the dust-lane, which was hitherto only hinted at. The near-IR to optical color baseline allows us to accurately assess the obscuring properties of this dust lane. Following De Koff[21] et al., we can infer a dust mass for this torus from:

$$M_{dust} = \frac{\sum <A_\lambda> [\text{mag}][\text{kpc}^2]}{6 \times 10^{-6} [\text{mag}][\text{kpc}^2][\text{M}_\odot]},$$ (2)

with the summation over the spatial extent of the obscuring material, and $<A_\lambda>$ the mean absorption in magnitudes. Based on this, we arrive at a $\sim 1 \times 10^4 \text{M}_\odot$ mass estimate for the dust-lane in 3C 452. This is about an order of magnitude less (at the same redshift) than dust-masses inferred for other 3C radio galaxies*, illustrating the usefulness of AO observations for morphological studies of the direct AGN environment.

3.2. Profile Analysis

Luminosity profiles and their derived quantities – effective radius (R_e), effective surface brightness (μ_e), mean surface brightness $(<\mu>)$, and their general shape are all important quantities for discriminating between various objects. Spiral galaxies usually have exponential profiles, whereas ellipticals are better fitted with de

---

*The dust-mass for 3C 452 listed in Table 2 of De Koff et al. is wrong.
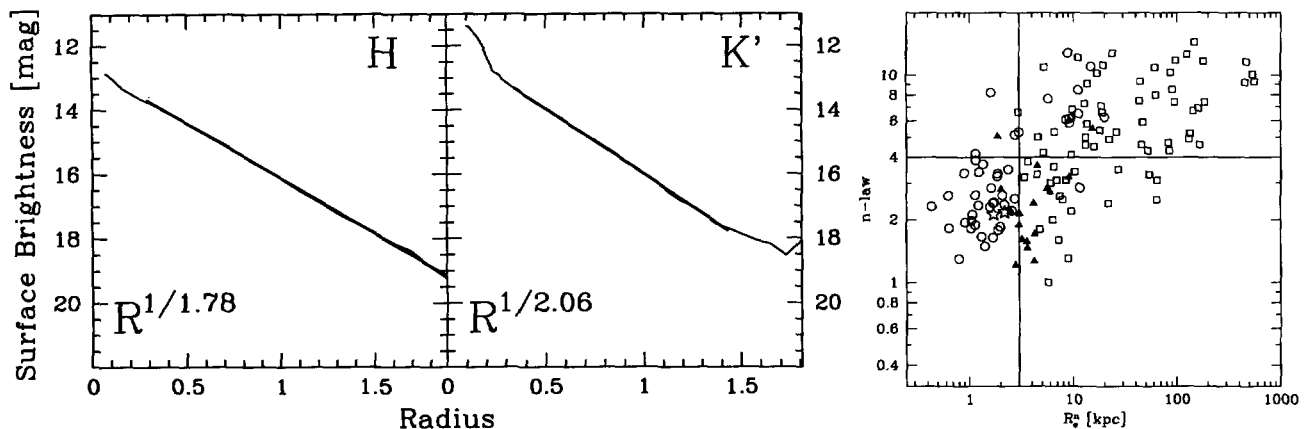
Figure 2. [Left Panel] Near-IR AO radial luminosity profiles of 3C 452, with their best fitting $R^{1/n}$ law overplotted. In the K'-band an unresolved nuclear component can be seen, something not visible in the H-band. [Right Panel] Plot of Effective Radius versus n-law index. Small ellipticals are in the lower left, large Brightest Cluster Galaxies to the upper right corner. The solid triangles are 3C radio galaxies (profiles measured with NICMOS[22]), and our AO source 3C 452 is indicated by the two open star symbols (H and K'-bands).

Vaucouleurs' type laws ($\mu(r) \propto R^{1/n}$). While the morphological differences between spirals and ellipticals are obvious and ellipticals as a class appear rather similar, they do exhibit significant differences in their profiles. For instance, Faber[6] et al. find a correlation between absolute luminosity and profile shape, in the sense that the more massive systems have shallower inner profiles. Less luminous ellipticals have profiles which lack this "core", and remain steep all the way up the resolution limit. The physical size scale of this cusp has been found to be on the order of 500 pc.[6,7] This "break radius" corresponds to about 0.35″ for 3C 452, or $\sim$ 20 pixels, enough for a detailed fit. Again, this would not have been possible at lower resolutions. First, we will fit the profile with a generalized de Vaucouleurs' law ($R^{1/n}$). This exponent n also correlates with elliptical type. Following Graham[23] et al., we define:

$$\mu(r) = \mu_0 + \frac{2.5 b_n}{\ln(10)} \left(\frac{r}{r_e} \right)^{1/n} \tag{3}$$

with r_e the scale radius, μ_0 the central surface brightness, and the constant b_n approximated by: $b_n \approx 2n - 0.327$. Note that in the $n = 1$ case the profile is exponential, and better represents spirals. The major axis luminosity profile of 3C 452 was fitted with this law, and the χ^2 minimized fitting values are given in Table 2. A literature sample of radio quiet ellipticals of varying size,[23,24] and powerful radio sources[22] is presented in Fig. 2, right panel. Our AO data on 3C 452 indicate that this is an intermediate sized elliptical, possibly towards the small end of the radio galaxy distribution. There is no indication, based on the profile, that it has undergone any

Table 2. 3C 452 Profile Results

n-law Fit

H-band	$n = 1.71 \pm 0.09$ $R_{\rm eff} = 2.12 \pm 0.01$ kpc
K'-band	$n = 2.19 \pm 0.04$ $R_{\rm eff} = 2.18 \pm 0.02$ kpc

Nuker law Fit

H-band	$\alpha = 0.94,\ \beta = 4.65,\ \gamma = 0.12,\ R_{\rm break} = 1.68$ kpc
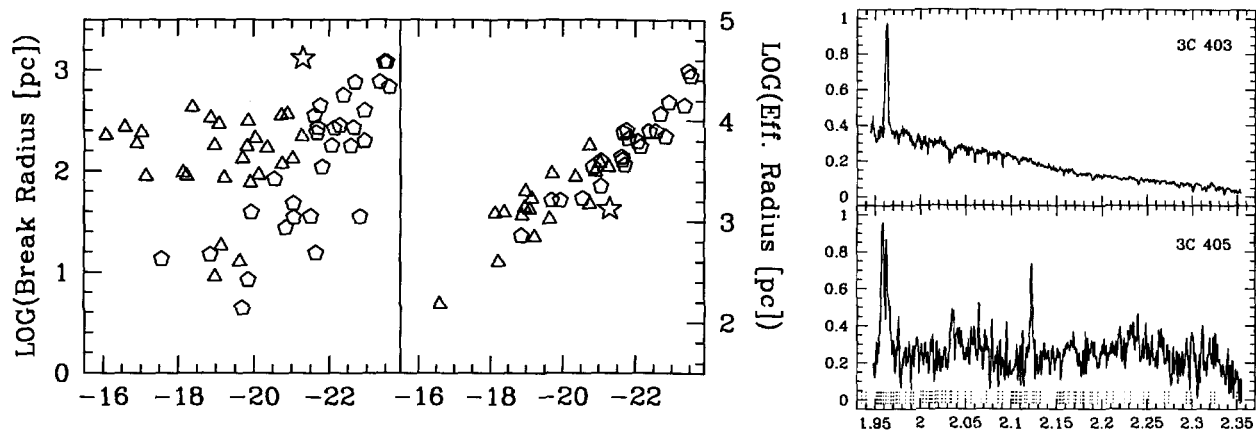
Figure 3. [Left Panel] 3C 452 (open star symbol) compared to low-redshift (HST observed) ellipticals.[6] Both the Break-radius and the Effective radius correlate with absolute luminosity. Open triangles: "steep" ellipticals ($\gamma < 0.3$), open pentagons: "core" ellipticals ($\gamma \geq 0.3$). [Right Panel] Near-IR AO spectra of 3C 403 and 3C 405, plotted in the source restframe with arbitrary flux units. Note the much higher S/N in the spectrum of 3C 403. Lines are identified in Table 3. The thin lines on the bottom of 3C 405's spectrum indicate the position of atmospheric OH lines.

major merger in its history: the profile lacks any hint of flattening towards the center. This seems to be a common trait among powerful radio galaxies.[22]

The four free parameters of the Faber[6] et al. profile law (coined "Nuker"-law) were fitted simultaneously using our χ^2 minimizing simulated-annealing code. Results are listed in Table 2. Consistent with our n-law fit, the source is classified as a "steep" source (indicated as open triangles in Fig. 3), albeit with a brighter host galaxy. This may be a selection effect though, since 3C 452 is at a much larger distance than the literature galaxies. The main purpose of this exercise is to demonstrate the feasibility of high resolution profile analysis on these distant objects, enlarging the time baseline against which to study evolutionary effects.

3.3. AGN Luminosity Contribution

As can be seen in Fig. 2 (left panel), any deviation from the smooth n-law profile will stand out. Of particular interest is the nuclear (AGN) contribution to the total. By extrapolating the n-law inwards, we can estimate the AGN contribution by measuring the excess emission over the n-law. We actually performed a χ^2 minimization of a variable pointsource contribution to the profile shape, i.e., the goodness-of-fit was given by the least deviation from a perfect n-law profile. The results are listed in Table 2. For our spectroscopy program, it was necessary that the AGN would not contribute too much to the nuclear emission, because it might wash out the stellar absorption signature we were trying to measure. It is clear that with just a 4% PSF contribution in the K'-band this condition is satisfied.

4. SPECTROSCOPY

The original idea was to combine the very high spatial resolution and the near-IR capability of the NIRSPEC instrument to measure the exact slope of the ^{12}CO bandhead at $2.293\mu m$ restframe. This method has been successfully applied before,[16] and since this line is formed in outer envelopes of cool stars, it provides a clean measure of the *stellar* velocity dispersion, and is not affected by thermal broadening: the slope of the bandhead becomes more shallow with an increase of the velocity dispersion of the stars. With NIRSPEC-AO and its complement of very small slits, we would be able to obtain spectra of the region very close to the nucleus, a region presumably gravitationally influenced by the central massive black hole (the slit width of $0.072''$ corresponds to $\sim$100 pc at the redshift of 3C 452).
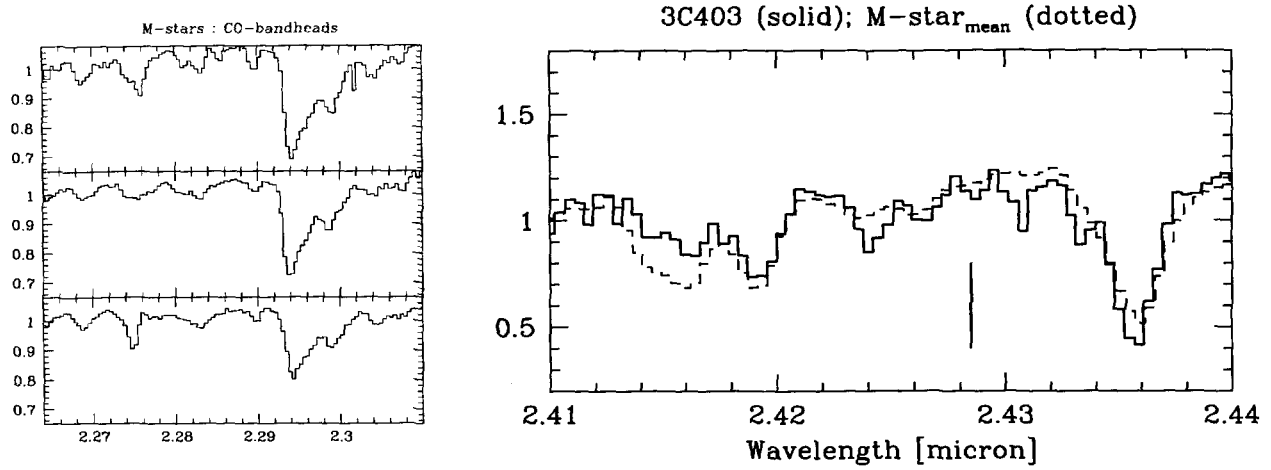
Figure 4. [Left Panel] ^{12}CO bandheads as detected in our M-type template stars. [Right Panel] Actual spectral region of 3C 403 (the radio source with the highest S/N spectrum) which should contain the redshifted bandhead (marked with the vertical line). A mean M-star spectrum is overplotted. No hint of a bandhead is present in 3C 403.

Unfortunately, the spectroscopic data on 3C 405 and 3C 452 do not have the required S/N. The one source with enough S/N (3C 403) does not exhibit any sign of a CO bandhead at its correct (redshifted) position (cf. Fig. 4, right panel). The instrumental setup clearly was able to measure bandheads (left panel), so in the case of 3C 403 it might be central obscuration that hides this spectral signature. This (more or less uniform) obscuration is hinted at in the colormap of Fig. 1, right panel.

4.1. Emission Lines

Though not strictly needing AO, we did measure several emission lines in 3C 403 and 3C 405 (3C 452 did not have any, at least not to the level detected). The measurements are listed in Table 3. The high excitation line [Si VI], due to either UV irradiation by the central AGN, or to powerful shocks close to the AGN, is

Table 3. Near-IR emission lines

3C 403

Line	λ	FWHM	σ [km/s]	Redshift
Br-δ 19451Å	20591Å			0.0586
[Si VI] 19629Å	20777Å	35.4Å	218	0.0585
[Ca VIII] 23211Å	24569Å			0.0585

3C 405

Line	λ	FWHM	σ [km/s]	Redshift
H$_2$ 1-0S(3) 19576Å	20684Å	34.5Å	213	0.0566
[Si VI] 19629Å	20746Å	35.3Å	217	0.0569
H$_2$ 1-0S(2) 20338Å	21489Å			0.0566
H$_2$ 1-0S(1) 21218Å	22417Å	19.4Å	110	0.0565

NOTE – FWHM's have been corrected for the instrumental resolution of 12.7Å.

present in both spectra, with almost identical widths. It should be noted that these widths (as σ in km/s) are very compatible with stellar velocity dispersions as measured for radio galaxies,[25] but not necessarily due to gravitational motion.

5. SUMMARY

We demonstrated the potential AO observations have to radio galaxy host studies. It equals, and complements, HST's optical imaging in terms of resolution, extending the realm of detailed nuclear environment imaging into the near-IR. The spectroscopic setup we used (NIRSPEC + KECK) was not ideally suited for our project, however. When working close to the diffraction limit, even 10m class telescopes are photon starved.

Based on this pilot study, AO imaging (and perhaps AO spectroscopy) on a large, and systematically set up sample can significantly further our knowledge of these large galaxies and their massive black holes.

ACKNOWLEDGMENTS

REFERENCES

1. S. Lilly, "Discovery of a radio galaxy at a redshift of 3.395," *Astroph. Journal* **333**, p. 161, 1988.
2. W. J. M. van Breugel, S. A. Stanford, H. Spinrad, and et al., "Morphological evolution in high-redshift radio galaxies and the formation of giant elliptical galaxies," *Astroph. Journal* **502**, p. 614, 1998.
3. L. Cowie, E. M. Hu, A. Songaila, and E. Egami, "The evolution of the distribution of star formation rates in galaxies," *Astroph. Journal* **481**, p. L9, 1997.
4. H. Spinrad, A. Dey, D. Stern, and et al., "Lbds 53w091: an old, red galaxy at z=1.552," *Astroph. Journal* **484**, p. 581, 1997.
5. P. McCarthy, "High redshift radio galaxies," *Ann. Rev. Astr Astroph* **31**, p. 639, 1993.
6. S. M. Faber, S. Tremaine, E. A. Ajhar, and et al., "The centers of early-type galaxies with hst. iv. central parameter relations.," *Astron. Journal* **114**, p. 1771, 1997.
7. T. R. Lauer, E. A. Ajhar, Y.-I. Byun, and et al., "The centers of early-type galaxies with hst.i.an observational survey," *Astron. Journal* **110**, p. 2622, 1995.
8. Y.-I. Byun, C. J. Grillmair, S. M. Faber, and et al., "The centers of early-type galaxies with hst. ii. empirical models and structural parameters," *Astron. Journal* **111**, p. 1889, 1996.
9. T. L. Hill, C. A. Heisler, R. Sutherland, and R. W. Hunstead, "Starburst of seyfert? using near-ir spectroscopy to measure the activity in composite galaxies," *Astron. Journal* **117**, p. 111, 1999.
10. L. Vanzi, A. Alonso-Herrero, and G. H. Rieke, "Near-ir spectroscopy of arp interacting galaxies," *Astroph. Journal* **504**, p. 93, 1998.
11. J. H. Black and E. F. van Dishoeck, "Fluorescent excitation of interstellar h2," *Astroph. Journal* **322**, p. 412, 1987.
12. R. J. Rudy, R. C. Puetter, and S. Mazuk, "Paschen lines and the reddening of the radio galaxy 3c 109," *Astron. Journal* **118**, p. 666, 1999.
13. R. J. Thornton, A. Stockton, and S. Ridgway, "Optical and near-infrared spectroscopy of cygnus a," *Astron. Journal* **118**, p. 1461, 1999.
14. J. H. Rhee and J. E. Larkin, "Probing the dust obscuration in seyfert galaxies using infrared spectroscopy," *Astroph. Journal* **538**, p. 98, 2000.
15. N. I. Gaffney, D. F. Lester, and G. Doppmann, "Measuring stellar kinematics in galaxies with the near-infrared (2-0) ^{12}co absorption bandhead," *Publ. Astron. Soc. of the Pacific* **107**, pp. 68–76, 1995.

16. T. Boeker, R. P. van der Marel, and W. D. Vacca, "Co band head spectroscopy of ic 342: Mass and age of the nuclear star cluster," *Astron. Journal* **118**, p. 831, 1999.

17. K. Gebhardt, R. Bender, G. Bower, and et al., "A relationship between nuclear black hole mass and galaxy velocity dispersion," *Astroph. Journal* **539**, p. L13, 2000.

18. L. Ferrarese and D. Merritt, "A fundamental relation between supermassive black holes and their host galaxies," *Astroph. Journal* **539**, p. L9, 2000.

19. A. Quirrenbach, J. E. Roberts, K. Fidkowski, W. de Vries, and W. van Breugel, "Keck adaptive optics observations of the radio galaxy 3c 294: A merging system at z=1.786?," *Astroph. Journal* **556**, p. 108, 2001.

20. J. E. larkin, T. M. Glassman, and et al., "Exploring the structure of distant galaxies with adaptive optics on the keck ii telescope," *Publ. Astron. Soc. of the Pacific* **112**, pp. 1526–1531, 2000.

21. S. de Koff, P. Best, S. A. Baum, and et al., "The dust-radio connection in 3cr radio galaxies," *Astroph. Journal Suppl. Series* **129**, p. 133, 2000.

22. W. H. de Vries, C. P. O'Dea, and et al., "Hubble space telescope nicmos observations of the host galaxies of powerful radio sources: Does size matter?," *Astron. Journal* **120**, p. 2300, 2000.

23. A. Graham, T. Lauer, M. Colless, and M. Postman, "Brightest cluster galaxy profile shapes," *Astroph. Journal* **465**, p. 534, 1996.

24. N. Caon, M. Capaccioli, and M. D'Onofrio, "On the shape of the light profiles of early type galaxies," *Montly Notices of the Royal Astron. Soc.* **265**, p. 1013, 1993.

25. D. Bettoni, R. Falomo, F. Govoni, M. Salvo, and R. Scarpa, "The fundamental plane of radio galaxies," *Astr. & Astroph* **380**, p. 471, 2001.